Available online at www.sciencedirect.com

SCIENCE DIRECT®

International Journal of Solids and Structures 43 (2006) 4047–4062

INTERNATIONAL JOURNAL OF SOLIDS and STRUCTURES

www.elsevier.com/locate/ijsolstr

# An example of double forces taken from structural analysis

I. Vardoulakis [a,*], A.E. Giannakopoulos [b]

[a] *Faculty of Applied Mathematics and Physics, Department of Mechanics, National Technical University of Athens, Zographou Campus, Athens 15773, Greece*

[b] *Department of Civil Engineering, University of Thessaly, Volos 38336, Greece*

Received 19 April 2005
Available online 23 June 2005

**Abstract**

The classic Bernoulli–Euler beam is revisited in relation to the Timoshenko beam, using a T-type cross-section. A practical example of double forces is worked out, where the double forces appear due to the shearing of the horizontal flange of the T-section. It is shown that a non-local estimate of the mean value of the vertical deflection of the beam leads to a shear gradient that is energetically consistent with the double force. Therefore, an additional energy term that includes the derivative of the beam's curvature leads to a consistent non-local beam model, simple enough to be used in structural analysis. Such beam models are useful in micro- and nano-technology. Moreover, this simple example opens the discussion for the importance of non-local differentiation in the averaging theories of Mechanics.


*Keywords:* Double-forces; Beam theories; Gradient theories; Micro-electro-mechanical devices; Non-local differentiation; Averaging theories

## 1. Introduction

In case when a field varies locally linearly, we may identify it with its mean value over the considered averaging length, because the mean value of a linearly varying field in a sampling interval is equal to the value of it in the *mid-point* of the interval. Field theories where local values are identified with mean values are called *simple theories* and the corresponding continua, *locally homogeneous*. In case however where the field in the considered sampling interval is not described satisfactorily by a linear function, then of course

* Corresponding author. Tel.: +30 2421074179; fax: +30 242107169.
*E-mail addresses:* i.vardoulakis@mechan.ntua.gr (I. Vardoulakis), agiannak@uth.gr (A.E. Giannakopoulos).

0020-7683/$ - see front matter 
doi:10.1016/j.ijsolstr.2005.04.023

we have to assume that at least it possesses some curvature. In this case the averaging must be corrected accordingly, since a linear fit of the data does not suffice for the satisfactory description of the field locally. Thus for a ‘quadratically’ varying field, we have to approximate it by a two-term Taylor series expansion around each special point, so as to incorporate the effect of the curvature. Field theories based on averaging rules that include the effect of higher gradients are called *higher gradient theories*.

Averaging considerations find many applications in continuum mechanics. In the frame of the engineering beam-bending theory, it is well known that a locally linear approximation of the vertical deflection $w(x)$ is not sufficient. In the case of pure bending we approximate $w(x)$ by a two-term Taylor series expansion around a point $x = 0$ along the beam $x$-axis

$$w(x) \approx w(0) + \left(\frac{\mathrm{d}w}{\mathrm{d}x}\right)_{x=0} x + \frac{1}{2}\left(\frac{\mathrm{d}^2 w}{\mathrm{d}x^2}\right)_{x=0} x^2 = w_0 - \psi x - \frac{1}{2}\kappa x^2 \tag{1}$$

In this case the deformation is not locally homogeneous. For the estimation of the curvature $\kappa$ we need at least three measurements (at $x$ and $x \pm \Delta x$) and a parabolic interpolation of the data, Fig. 1.

Accordingly, the engineering bending theory of long prismatic beams is described by a constitutive relation, which connects the bending moment $M$ to the curvature $\kappa = 1/R$ of the deflection of the beam,

$$M = M(\kappa) \tag{2}$$

For a beam segment of length $\ell$ with $-\ell/2 \leqslant x \leqslant \ell/2$, the average deflection at its mid-point $x = 0$ is

$$\langle w \rangle|_{0,\ell} = \frac{1}{\ell}\int_{-\ell/2}^{\ell/2}\left(w_0 - \psi\xi - \frac{1}{2}\kappa\xi^2\right)\mathrm{d}\xi = w_0 - \frac{1}{24}\ell^2\kappa \tag{3}$$

where

$$\kappa = -\left.\frac{\mathrm{d}^2 w}{\mathrm{d}x^2}\right|_0 \approx \frac{24}{\ell^2}\left(w_0 - \langle w \rangle|_{0,\ell}\right) \tag{4}$$

This means that the engineering beam-bending theory is a 2nd gradient continuum theory that accounts for the effect of the deviation of the local deflection from its mean value over an arbitrary, but sufficiently small, sampling length.

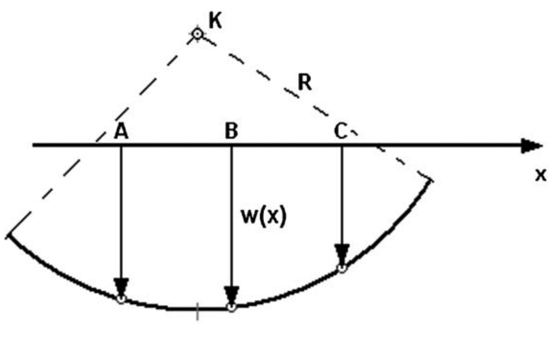


Fig. 1. Three point interpolation of the bending line.

## 2. A simple 2nd gradient structural model

It is well known that the Bernoulli–Euler bending theory of beams is essentially flawed, since it contains a contradiction as far as the computation of shear forces is concerned. Indeed within such a theory we get that in meso-structural scale (i.e. over the surface of a cross-section) the relation between shear stress and shear strain is given as

$$\tau = G\gamma, \quad \gamma = \frac{\mathrm{d}w}{\mathrm{d}x} + \psi \tag{5}$$

where $w(x)$ is the vertical displacement and $\psi(x)$ the rotation angle of the cross-section of the beam at position $x$. Eq. (5) implies homogeneous linear and isotropic material response of the beam and so $G$ is the shear modulus ($G = E/(2(1+v))$; $E$ is the elastic modulus and $v$ is Poisson's ratio).

Assuming that the cross-section perpendicular to the undeformed axis remains perpendicular to the deformed axis of the beam, we get

$$\psi = -\frac{\mathrm{d}w}{\mathrm{d}x} \tag{6}$$

This assumption together with the above elasticity equation for the shear stresses on the cross-section stands in contradiction to the existence of finite shear forces,

$$Q = \int_A \sigma_{xz}\,\mathrm{d}A \tag{7}$$

where the integral extends over the whole surface $A$ of the normal to the axis section of the beam. In order to remedy this contradiction, some authors claimed that the Bernoulli–Euler theory is only true for the so-called shear-stiff beam; i.e. for a beam with infinite shear modulus

$$G = \frac{E}{2(1+v)} \to \infty \quad \text{(Poisson's ratio } v = -1) \tag{8}$$

However, this assumption is not necessary, since one may derive the Bernoulli–Euler theory as a limiting case of the so-called Timoshenko beam theory (Timoshenko, 1921).[1] In the later case the set of governing equations consists of the moment equilibrium equation

$$-Q + \frac{\mathrm{d}M}{\mathrm{d}x} = 0 \tag{9}$$

and the two constitutive equations on a macro-structural level for the bending moment $M(x)$ and shear force $Q(x)$,

$$\begin{aligned} M &= (EI)\frac{\mathrm{d}\psi}{\mathrm{d}x} \\ Q &= (GA_s)\gamma = (GA_s)\left(\psi + \frac{\mathrm{d}w}{\mathrm{d}x}\right) \end{aligned} \tag{10}$$

where $I$ is the moment of inertia of the section

$$I = \int_A y^2\,\mathrm{d}A \tag{11}$$

[1] The finite element users often encounter severe "locking" of the beam elements due to (8).

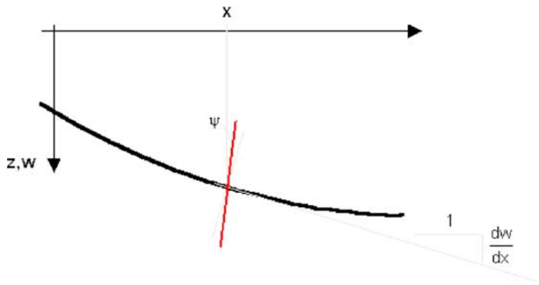


Fig. 2. The Timoshenko beam.

and $A_s$ is defined as a suitable fraction of the total cross-sectional area (cf. Eq. (13)). Fig. 2 shows the Timoshenko beam, where we notice that the cross-section normal to the undeformed axis does not remain normal to the deformed axis of the beam.

We introduce the following non-dimensional quantities:

$$\xi = \frac{x}{L}, \quad \omega = \frac{w}{L}, \quad \eta^2 = \frac{EI}{GA_s L^2} \tag{12}$$

where $L$ is a characteristic macro-structural length of the beam, which depends on the load distribution and type of supports (e.g. the distance between two simple supports or the length of a cantilever beam with vertical load at the end). The number $\eta$ depends on the selection of the '*statically effective*' area of the cross-section,

$$A_s = kA \quad (k \geqslant 1) \tag{13}$$

$A_s$ is calibrated in such a way that the result of the enhanced Timoshenko theory produces the same result in terms of deflection, as an energy method would do, which considers the contribution of the vertical shear stresses $\sigma_{xz}$ in the elastic energy of the beam. For example, for a rectangular cross-section with height $H$, Timoshenko (1921) predicts

$$\eta^2 = \frac{1}{5}(1+\nu)\left(\frac{H}{L}\right)^2 \ll 1 \quad \text{for } H < L \tag{14}$$

We remark that the number $\eta$ essentially compares the meso-structural length $H$ to the macro-structural length $L$. A notable case arises for beams made of auxetic composites (e.g. certain foams) where $\nu \to -1$ and so $\eta \to 0$.

With the notation as in Eq. (12), the bending moment equilibrium equation becomes[2]

$$\left(1 - \eta^2 \frac{d^2}{d\xi^2}\right)\psi = -\frac{d\omega}{d\xi} \;\Rightarrow\; \psi \approx -\left(1 + \eta^2 \frac{d^2}{d\xi^2}\right)\frac{d\omega}{d\xi} \tag{15}$$

Based on the remarks presented in the Introduction, related to averaging, Eq. (15) is re-interpreted as follows: The original Bernoulli–Euler hypothesis pertaining to the assumption that cross-sections remain perpendicular to the beam axis, Eq. (6), is replaced by a weaker statement which refers to the mean value of the slope of the deflection curve

$$\psi = \left\langle -\frac{dw}{dx} \right\rangle \tag{16}$$

[2] Cf. Appendix A.

For long prismatic beams, in the sense that $\eta < 1$, we recover the Bernoulli–Euler beam theory as an approximation of the Timoshenko beam theory,

$$\psi = -\frac{dw}{dx} + O(\eta^2) \tag{17}$$

$$M = (EI)\kappa, \quad \kappa = \frac{d\psi}{dx} \approx -\frac{d^2w}{dx^2} \tag{18}$$

$$Q = (GA_s)\gamma, \quad \gamma = \frac{dw}{dx} + \psi \approx \eta^2 L^2 \frac{d^3\omega}{dx^3} \Rightarrow Q \approx (EI)\frac{d\kappa}{dx} \tag{19}$$

## 3. The T-beam

### 3.1. The concept of double-force

In the previous sections we dealt with the familiar concepts of shear force and bending moment. In this section we present an example taken from Structural Analysis that has helped us to understand better the somehow elusive concept of "double force", which is used in the presentation of 2nd gradient Continuum theories (cf. Mindlin, 1964).

We consider a beam under the action of loads acting in the direction of the vertical $z$-axis. The beam has a symmetric thin-walled cross-section, in the form of a T-shaped section, as shown in Fig. 3.

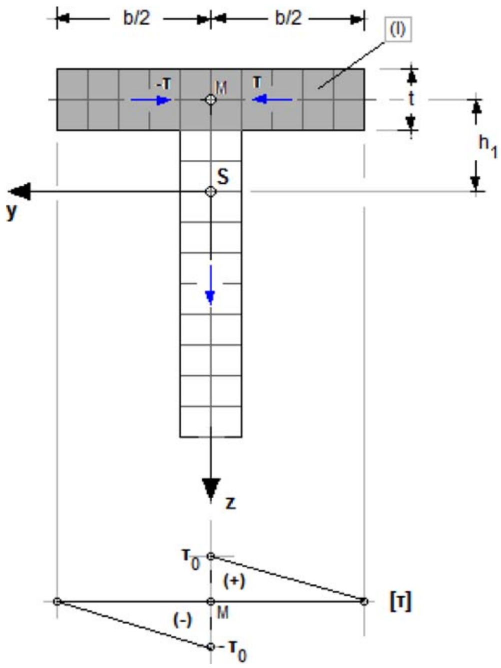


Fig. 3. The T-beam section and the shear stress distribution $\sigma_{xy}$ along the horizontal plate (I). The point M is the shear center of the beam. The point S is the area center of the cross-section.

According to the theory of shear for thin-walled sections, we have that along the horizontal plate (I) of the T-section, shear stresses develop

$$\sigma_{xy} = \tau(y) = \begin{cases} -\tau_0\left(1 - \frac{y}{b/2}\right), & 0 < y \leqslant b/2 \\ +\tau_0\left(1 + \frac{y}{b/2}\right), & -b/2 \leqslant y < 0 \end{cases} \tag{20}$$

where

$$\tau_0 = \frac{b/2}{W_1}\frac{\mathrm{d}M_y}{\mathrm{d}x}, \quad W_1 = \frac{I_{yy}}{h_1} \tag{21}$$

In Eq. (21), $I_{yy}$ is the moment of inertia of the beam around the $y$-axis, $M_y$ is the bending moment in the $y$-axis and $h_1$ is the distance of the horizontal plate (I) from the area center $S$ of the cross-section.

This shear stress distribution gives rise to the action of a force-doublet $(Q_{y\ell}, Q_{yr})$, which is acting at the points $L$ and $R$, to the left and to the right of the shear enter $M$ and at distances $b/6$ from the symmetry axis; Fig. 4. This force-doublet is a system of self-equilibrating forces, with

$$Q_{yr} = -Q_{y\ell} = \widetilde{Q}_y = \frac{1}{4}(bt)\tau_0 \tag{22}$$

To the above shear-stress distribution along the plate (I) we assign a shear-strain field, that is given according to Hooke's law as follows:

$$\gamma_{xy} = \frac{\sigma_{xy}}{G} = \frac{\tau_0}{G}\begin{cases} -\left(1 - 2\frac{y}{b}\right), & 0 < y \leqslant b/2 \\ +\left(1 + 2\frac{y}{b}\right), & -b/2 \leqslant y < 0 \end{cases} \tag{23}$$

The corresponding elastic shear strain-energy density and the axial distribution of this type of energy is

$$e_{(\mathrm{I})} = \frac{1}{2}G\gamma_{xy}^2 \Rightarrow E_{\ell Q_y} = 2t\int_0^{b/2} e_{(\mathrm{I})}\mathrm{d}y = \frac{1}{2}\frac{bt}{3}\frac{\tau_0^2}{G} \tag{24}$$

$E_{\ell Q_y}$ is the linear elastic strain energy due to shear of the plate (I), i.e. its cross-section average. In order to interpret Eq. (24), we define the shear-strain gradient:

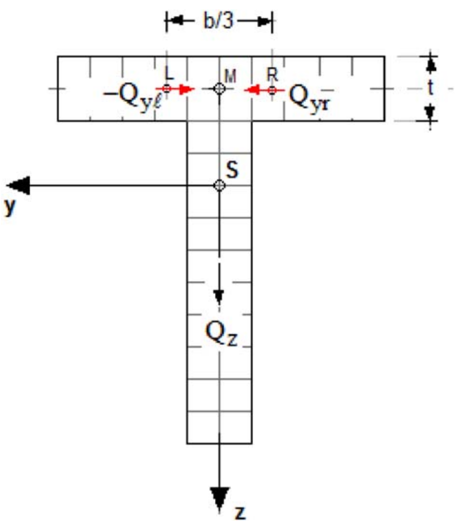


Fig. 4. The force doublet acting at the centers L and R of the shear stress distribution $\sigma_{xy}$ along the horizontal plate (I).

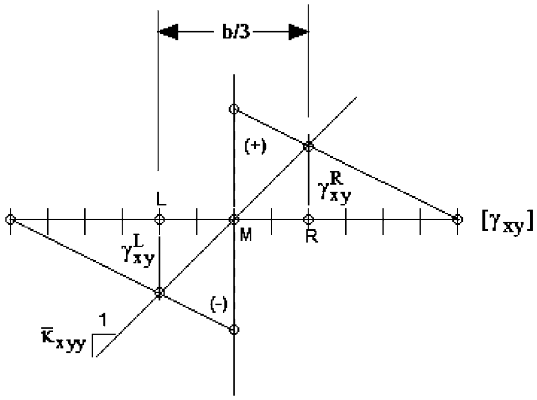


Fig. 5. A geometric construction of the generalized derivative of the shear strain at the shear center M.

$$\kappa_{xyy} = \frac{\partial}{\partial y}\gamma_{xy} \tag{25}$$

We remark that the strain field is discontinuous at the shear center $M$ ($y = 0$). In order to compute the generalized gradient of the shear strain at the shear center, we evaluate the strain at the collocation points L and R, which are the centroids of corresponding distributions to the left and to the right of the shear center M:

$$\begin{aligned} \gamma^L_{xy} &= \gamma_{xy}|_{y=\frac{b}{6}} = \frac{\tau_0}{G(b/2)}\left(-\frac{1}{3}b\right) \\ \gamma^R_{xy} &= \gamma_{xy}|_{y=-\frac{b}{6}} = \frac{\tau_0}{G(b/2)}\left(+\frac{1}{3}b\right) \end{aligned} \tag{26}$$

At this point, we define the generalized derivative of the shear strain at the point M as (Fig. 5):

$$\bar{\kappa}_{xyy} = \frac{\gamma^L_{xy} - \gamma^R_{xy}}{(LR)} = -2\frac{\tau_0}{G(b/2)} \tag{27}$$

In Appendix B, we derive Eq. (27) through an asymptotic plate theory that models the shearing of plate (I).

We define now a measure for the force doublet $(\vec{Q}_{y\ell}, \vec{Q}_{yr})$, the so-called double-force, with dimensions of a force moment

$$M_{xyy} = -\widetilde{Q}_y\frac{b}{3} = -\frac{1}{12}\tau_0 t b^2 \tag{28}$$

and hypothesize that

$$E_{\ell Q_y} = \frac{1}{2}M_{xyy}\bar{\kappa}_{xyy} \tag{29}$$

Indeed, by substituting Eqs. (27) and (28) into (29), we can verify that Eq. (24) holds true.

We observe also that

$$M_{xyy} = \left(G\frac{b^3 t}{48}\right)\bar{\kappa}_{xyy} \tag{30}$$

or with the notation

$$I' = \frac{b^3 t}{48} \tag{31}$$

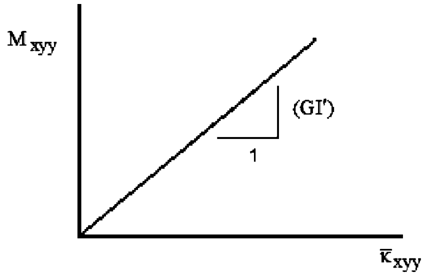


Fig. 6. The constitutive relation between the force doublet and the generalized shear strain gradient.

we get the constitutive relation for the considered double force (Fig. 6),

$$M_{xyy} = (GI')\bar{\kappa}_{xyy} \tag{32}$$

Eq. (32) is analogous to the one of the ordinary beam-bending theory that relates the bending moment $M_y$ to the curvature $\kappa = -\frac{d^2w}{dx^2}$,

$$M_y = (EI_{yy})\kappa \tag{33}$$

The constitutive relation (32) gives rise to the following definition of the double force as the moment of shear stresses:

$$M_{xyy} = \int_{(\mathrm{I})} y\sigma_{xy}\,dA \tag{34}$$

Indeed, if we evaluate Eq. (34), with Eq. (20) for the shear stresses, we obtain Eq. (28). To summarize, the main results so far are: The measures of the double force, Eq. (28), the generalized shear gradient, Eq. (27), and their energy linear distribution, Eq. (24).

### 3.2. The physical interpretation of $\bar{\kappa}_{xyy}$

With Eq. (21), Eq. (28) becomes

$$M_{xyy} = -\frac{1}{24}\frac{b^3th_1}{I_{yy}}\frac{dM_y}{dx} \tag{35}$$

Replacing Eq. (35) into (32), we obtain

$$\bar{\kappa}_{xyy} = \frac{1}{GI'}M_{xyy} = -2h_1\frac{1}{GI_{yy}}\frac{dM_y}{dx} \tag{36}$$

which we combine with the curvature-moment constitutive equation of the beam-bending theory, Eq. (33), yielding

$$\bar{\kappa}_{xyy} = -4(1+\nu)h_1\frac{d\kappa}{dx} \tag{37}$$

Thus, the kinematic quantity $\bar{\kappa}_{xyy}$ is proportional to the derivative of the curvature along the beam axis.

We define[3]

$$\bar{\kappa}' = \bar{\kappa}_{xyy} = -\ell_c\frac{d\kappa}{dx}, \quad \ell_c = 4(1+\nu)h_1 \tag{38}$$

[3] It is obvious from Eq. (38) that the shear stiff beam is a bad model.

and the linear elastic strain-energy density (energy per unit beam length) becomes

$$E_\ell = \frac{1}{2}(EI_{yy})\kappa^2 + \frac{1}{2}(GA_s)\gamma + \frac{1}{2}(GI')\ell_c^2\left(\frac{\mathrm{d}\kappa}{\mathrm{d}x}\right)^2 \tag{39}$$

with

$$\begin{aligned}\gamma &\approx -\eta^2\ell^2\frac{\mathrm{d}^3w}{\mathrm{d}x^3}\\ \eta^2\ell^2 &= \frac{(EI_{yy})}{GA_s}\end{aligned} \tag{40}$$

and from

$$\kappa \approx -\frac{\mathrm{d}^2w}{\mathrm{d}x^2} \quad \Rightarrow \quad \frac{\mathrm{d}^3w}{\mathrm{d}x^3} \approx -\frac{\mathrm{d}\kappa}{\mathrm{d}x} \tag{41}$$

Eq. (39) becomes

$$E_\ell = \frac{1}{2}(EI_{yy})\kappa^2 + \frac{1}{2}(GA_s)\ell^2\kappa'^2 + \frac{1}{2}(GI')\ell_c^2\kappa'^2 \tag{42}$$

In other words, the work of shear forces doublet is effective in cases of non-pure bending, where the curvature is not constant. The effects of the shear force $\vec{Q}_z$, acting along the stem, and the shear-force doublet $(\vec{Q}_{y\ell}, \vec{Q}_{yr})$, which is acting along the plate (I), appear separately in the last two terms of Eq. (42), and both are related to the derivative $\kappa' = (\mathrm{d}\kappa/\mathrm{d}x)$ of the curvature. Note that the first and third terms in the r.h.s of Eq. (39) have the form of the Bernoulli–Euler beam within the theory of gradient elasticity, which has been treated thoroughly by Papargyri-Beskou et al. (2003).

### 3.3. The mathematical meaning of $\bar{\kappa}_{xyy}$

From

$$M_{xyy} = \int_{(\mathrm{I})} y\sigma_{xy}\,\mathrm{d}A = G\int_{(\mathrm{I})} y\gamma_{xy}\,\mathrm{d}A \tag{43}$$

and Eq. (32), we obtain the (generalized) strain gradient $\bar{\kappa}_{xyy}$ as

$$\bar{\kappa}_{xyy} = \frac{1}{I'}\int_{(\mathrm{I})} y\gamma_{xy}\,\mathrm{d}A \tag{44}$$

We observe that Eq. (44) is dual to the definition of the double-force, Eq. (43). We can show by inspection that Eq. (44) is equivalent to Eq. (27).

The above results suggest that for the anti-symmetric distributions, such as

$$\gamma_{xy} = \gamma(y) = \frac{\tau_0}{G}\begin{cases}\left(1 + 2\frac{y}{b}\right), & -1/2 \leqslant y/b \leqslant 0\\ \left(-1 + 2\frac{y}{b}\right), & 0 < y/b \leqslant 1/2\end{cases} \tag{45}$$

which are discontinuous at the shear center $M$ $(y = 0)$, the geometric construction shown in Fig. 5 can be presented as

$$\bar{\kappa}_{xyy} = \frac{\gamma_{xy}(\bar{y})}{\bar{y}} \tag{46}$$

with

$$\bar{y} = \frac{\int_0^{b/2} y\gamma_{xy}\,\mathrm{d}y}{\int_0^{b/2} \gamma_{xy}\,\mathrm{d}y} \tag{47}$$

In Appendix C we show that for a discontinuous function such as the one given through Eq. (45), a Riemann–Liouville type of derivative can be formulated.

## 4. Practical considerations and applications to micro-electro-mechanical devices

It is important to examine when the energy per-unit-length term due to double-force becomes comparable to the main (bending) term in Eq. (39). Using the T-beam configuration, with the notation of Fig. B.1 and the results of Appendix B, we get

$$\frac{\frac{1}{2}(GI')\ell_c^2\left(\frac{\mathrm{d}\kappa}{\mathrm{d}x}\right)^2}{\frac{1}{2}(EI_{yy})\kappa^2} = \frac{Q_z^2}{M_y^2}\frac{(1+v)}{2}\frac{b^2\frac{e}{b}}{\frac{h}{t}\left(\frac{e}{b}\frac{h}{t}+2\right)^2} \tag{48}$$

For a cantilever beam of length $\ell$ with a concentrated force at the free end,

$$\frac{Q_z^2}{M_y^2} = \ell^2 \tag{49}$$

and with that Eq. (48) becomes

$$\frac{\frac{1}{2}(GI')\ell_c^2\left(\frac{\mathrm{d}\kappa}{\mathrm{d}x}\right)^2}{\frac{1}{2}(EI_{yy})\kappa^2} = \frac{b^2}{\ell^2}\frac{(1+v)}{2}\frac{\frac{e}{b}}{\frac{h}{t}\left(\frac{e}{b}\frac{h}{t}+2\right)^2} \tag{50}$$

If we assume that

$$\frac{eh}{bt} \ll 2 \tag{51}$$

then Eq. (50) is approximated by

$$\frac{\frac{1}{2}(GI')\ell_c^2\left(\frac{\mathrm{d}\kappa}{\mathrm{d}x}\right)^2}{\frac{1}{2}(EI_{yy})\kappa^2} = \frac{(1+v)}{8}\left(\frac{b}{\ell}\right)^2\frac{e/b}{h/t} \tag{52}$$

It is interesting to note that for low values of the ratio $(h/t)$, the energy term due to the double-force can become considerable. For example, taking $(e/b) = 1$, $v = 0$, $(h/t) = 1/16$ and $(b/\ell) = 1/4$, the double force energy is about 1/8 of the bending energy.

Periodic conducting lines (e.g. Al or Cu) which are patterned (e.g. etched) on insulating plates (e.g. Si wafers) are common in microelectronic devices. The internal stresses that develop in the conducting lines affect the passage of electric current. The experimental estimation of these stresses rely on measuring the curvature of the plates. A schematic of the line/plate system is shown in Fig. 7. Obviously, under proper conditions, the periodic cell shown in Fig. 7 resembles a T-beam and can be modeled as such. Typical dimensions of such configurations are $t = 500$ μm and $h = 1$ μm. Yeo et al. (1995) found that for thin lines, the experimental curvatures appear lower than those expected from the elastic analysis. Although this effect could be partly due to plasticity that develops in the conducting lines, the effect of strain gradient (enhanced due to the high ratio $t/h$) is also a possible explanation. The stiffer response of beams with energy representation as in Eq. (39) has been shown in detail by Papargyri-Beskou et al. (2003).

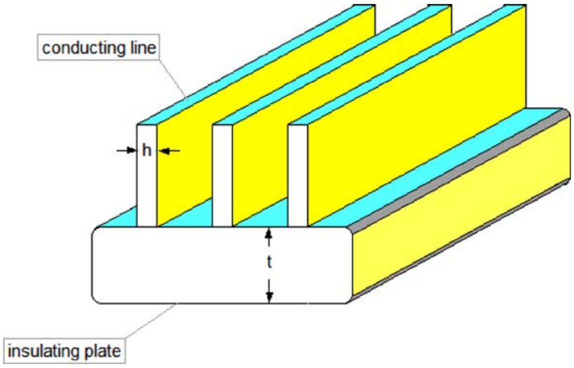


Fig. 7. Patterned metal lines on insulating plate (wafer) in microelectronic devices.

## 5. Conclusions

We have demonstrated an example of double-forces taken from the bending analysis of a beam with T-type cross-section. The double-force is related to the shear strains that develop on the horizontal flange of the beam. This in turn, gives rise to the construction of a generalized shear strain-gradient and connects through equilibrium the double force with the curvature-gradient of the beam. A novel characteristic length appears that scales with the distance of the shear center from the geometric center of the cross-section. At the end, a non-local beam theory is developed that accounts for an additional energy term of the curvature-gradient. The analysis can be extended easily to other types of thin-walled sections, homogeneous or inhomogeneous.

The newly found length, related to the gradient of the beam curvature, deserves a few additional comments. Suppose that an experimentalist is measuring load and deflection of cantilever T-beams of various lengths, loaded at their free ends with concentrated vertical forces. Then, even with a Tisoshenko beam model, there will be a stiffening effect for short beams, leading to a ‘‘length scale effect’’. The interesting point is that this length scale effect has a definite structural origin, other than a material one. Therefore, one has to be careful in interpreting length scale effects by assuming material parameters only. A detailed mechanical analysis can unravel the issue.

Returning to the double-force concept, our example shows that advanced continuum theories can be formulated by recognizing double-forces, which are energetically dual with generalized kinematic gradients. Such formulations are capable to describe small size structures, offering novel engineering methodologies to the design of micro-electro-mechanical devices and assisting in the interpretation of material properties in the micro-scale.

We should point out that according to Mindlin one has to assume that the micro-displacement can be expressed as a sum of products of specified functions of the local coordinates in the micro-volume, e.g. in the form of $u'_j = x'_k \psi_{kj}$ (cf. Mindlin, 1964, truncated Taylor series expansion, Eq. 1.6). The present example of the T-beam shows clearly that the deformation at the micro-element scale needs not be continuous. Indeed we expect that at the level of the micro-element the deformation to be to some degree always discontinuous. Moreover we should bring to the attention that within the so-called representative elementary volume (REV) there is not such a thing like a local point, in the vicinity of which one could expand a function as a Taylor series. If this were to be the case, then micro- and macro-scales would have been indistinguishable. This has been always appreciated in the sense that most researchers are talking about integral averages of various physical properties over the REV. However this idea was only used for the value of some property (e.g. the density) but not for the derivative of it. It seems, that the above example justifies the suggestion to use non-local derivatives within the REV, such as the Riemann–Liouville operator.

The above non-local differentiation will allow to differentiate strongly fluctuating properties by considering their overall trend within the REV. As an example we could refer here to the long standing controversy in granular mechanics (Bardet and Vardoulakis, 2001), where the application of a Cosserat continuum approach is criticized using the argument that, within the REV, the existence of a large population of rolling contacts (i.e. dipoles) introduces a non-smooth rotation field that is not differentiable to yield the local value of curvature. The non-local differentiation in the above sense, would naturally eliminate the effect of the rolling contacts and leave only the effect of the (dissipative) sliding contacts.

## Acknowledgment

The authors want to acknowledge the EU project *Degradation and Instabilities in Geomaterials with Application to Hazard Mitigation* (DIGA) in the framework of the Human Potential Program, Research Training Networks (HPRN-CT-2002-00220). The second author wants also to acknowledge the project "Fatigue of MEMS" that is ongoing in the Laboratory for Strength of Materials and Micromechanics of the Department of Civil Engineering, University of Thessaly.

## Appendix A. The Schrödinger operator

We consider the differential equation

$$(1 - \ell^2\nabla^2)\Psi = \Lambda \tag{A.1}$$

Notice that in the literature the operator

$$L_S = 1 - \ell^2\nabla^2 \tag{A.2}$$

is known as the *Schrödinger operator*.

We assume for simplicity the 1D-case ($\nabla^2 \equiv \frac{\partial^2}{\partial x^2}$). We assume also that the Fourier transforms of the functions $\Psi(x)$ and $\Lambda(x)$ as well as of their derivatives up to order two exist. In that case the functions $\Psi$ , $\Psi'$ and $\Psi''$ are continuous and $\Psi \to 0$ as $|x| \to \infty$; the same is assumed to hold also for $\Lambda(x)$.

Thus we set

$$\begin{aligned} Y(\alpha) &= E\{\Psi(x)\} = \int_{-\infty}^{+\infty} \Psi(x)\mathrm{e}^{-\mathrm{i}\alpha x}\,\mathrm{d}x, \quad L(\alpha) = E\{\Lambda\} = \int_{-\infty}^{+\infty} \Lambda(x)\mathrm{e}^{-\mathrm{i}\alpha x}\,\mathrm{d}x \\ \Psi(x) &= E^{-1}\{Y(\alpha)\} = \frac{1}{2\pi}\int_{-\infty}^{+\infty} Y(\alpha)\mathrm{e}^{\mathrm{i}\alpha x}\,\mathrm{d}\alpha, \quad \Lambda = E^{-1}\{L(\alpha)\} = \int_{-\infty}^{+\infty} L(\alpha)\mathrm{e}^{\mathrm{i}\alpha x}\,\mathrm{d}\alpha \end{aligned} \tag{A.3}$$

If we apply the Fourier Transformation on both sides of Eq. (A.1), we get

$$Y - \ell^2\alpha^2 Y = L \quad \Rightarrow \quad Y = \frac{L}{1-(\alpha\ell)^2} = (1 + (\alpha\ell)^2)L + \mathrm{O}((\alpha\ell)^4) \tag{A.4}$$

By applying the inverse Fourier transform on the last equation, we get

$$E^{-1}\{Y\} \approx E^{-1}\{L\} + \ell^2 E^{-1}\{\alpha^2 L\}$$

or

$$\Psi \approx \Lambda + \ell^2\frac{\mathrm{d}^2\Lambda}{\mathrm{d}x^2} \tag{A.5}$$

Under suitable circumstances the inversion of Eq. (A.1) is then

$$\Psi \approx (1 + \ell^2 \nabla^2) \Lambda$$

## Appendix B. Detailed derivation of the derivative of the shear strain at the center of shear of a T-beam

In the analysis, a generalized derivative of the shear strain at the center of shear of a T-beam was defined by Eq. (27). It is the purpose of the present appendix to show that the fore-mentioned derivative is almost exact, if we allow for a more refined elastic analysis of the T-beam in the lines of Timoshenko and Goodier (1970). In this context, the T-beam is treated in way closer to a full 3-D analysis by treating the horizontal flanges of the beam as two 2-D plates that are fixed on the vertical web of the beam. Noting that the region of interest is at the shear center M of the T-beam, we follow a standard asymptotic analysis assuming the 2-D plates to extend indefinitely in the $y$-direction, as in Fig. B.1. The beam is supposed to have a length $2\ell$, the vertical web is $2e$ long and has thickness $h$.

For simplicity, we assume a moment distribution along the length of the beam to vary sinusoidal, as it typically approximates a simply supported beam with uniformly distributed load,

$$M_y = M_0 \cos(\pi x/\ell) \tag{B.1}$$

where $M_0$ is the moment in the middle of the beam ($x = 0$).

Using Airy's stress function $\Phi$, Timoshenko and Goodier (1970) give the following solution:

$$\Phi = (F_1 \exp(-\pi y/\ell) + F_2(1 + (\pi y/\ell)) \exp(\pi y/\ell)) \cos(\pi x/\ell) \tag{B.2}$$

where $F_1$ and $F_2$ are constants with the dimension of a force, which can be found by minimizing the strain energy of the flange and of the web,

$$F_1 = \frac{\ell}{2\pi t} P_0, \quad F_2 = -\frac{1+v}{2} F_1 \tag{B.3}$$

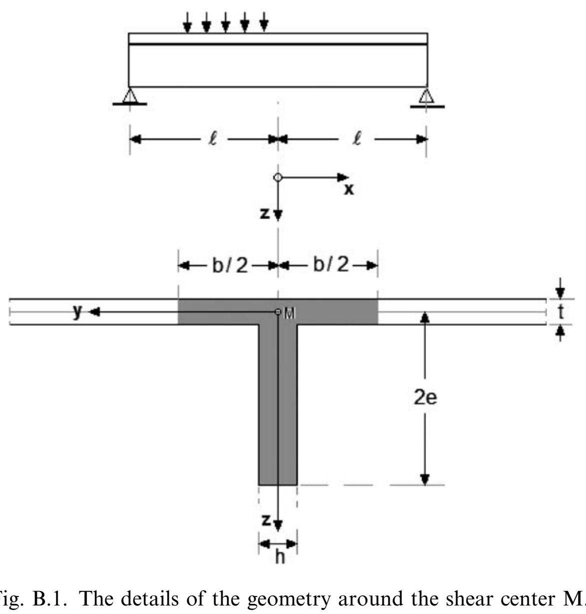


Fig. B.1. The details of the geometry around the shear center M.

with

$$P_0 = \frac{M_0}{e\left(1 + \frac{I_w}{A_w e^2} + \pi(3 + 2\nu - \nu^2)\frac{I_w}{te^2\ell}\right)}, \quad I_w = \frac{2}{3}e^3 h, \quad A_w = 2eh \tag{B.4}$$

In these expressions $\nu$ is Poisson's ratio of the beam, $A_w$ is the area of the web and $I_w$ is the area moment of the web.

The effective width of the flange $b$ can be obtained by applying the total equilibrium of moments to the T-beam through the axial stresses,

$$\sigma_{xx} = \frac{\partial^2 \Phi}{\partial x^2} \tag{B.5}$$

which act in the flange. This yields the following effective width of the flange:

$$b = \frac{4}{\pi(3 + 2\nu - \nu^2)}\ell \tag{B.6}$$

The shear stress

$$\sigma_{xy} = -\frac{\partial^2 \Phi}{\partial y \partial x} \tag{B.7}$$

relates by Hooke's Law with the shear strain as

$$\gamma_{xy} = \frac{\sigma_{xy}}{G} \tag{B.8}$$

where $G$ is the shear modulus of the beam.

Taking the $y$-derivative of the shear strain and evaluating it at the shear center $M(y = 0)$, after some algebra, we obtain

$$\left(\frac{\partial \gamma_{xy}}{\partial y}\right)_{y=0} = -\frac{1}{G}\frac{\mathrm{d}M_y}{\mathrm{d}x}\frac{3}{2e(2bt + eh)}\frac{3 + \nu}{3 + 2\nu - \nu^2} \tag{B.9}$$

It is of great interest to point that for $\nu \to -1$, the above form gives an infinite shear strain derivative, thus making the model inadequate (something that was found in the main analysis as well, but at a later stage). For $\nu = 0$, we obtain

$$\left(\frac{\partial \gamma_{xy}}{\partial y}\right)_{y=0} = -\frac{1}{G}\frac{\mathrm{d}M_y}{\mathrm{d}x}\frac{3}{2e(2bt + eh)} \tag{B.10}$$

which is exactly the result of Eq. (27), provided we replace in Eq. (21) the thin-wall approximations

$$\begin{aligned} h_1 &= \frac{e^2 t}{tb/2 + eh} \\ I_{yy} &= \frac{2}{3}e^3 h \frac{eh + 2bt}{tb/2 + eh} \end{aligned} \tag{B.11}$$

Clearly, for most common (positive) values of Poisson ratio (e.g. 1/3, 1/4), Eq. (B.9) is close to Eq. (27). The largest deviation occurs for near the incompressibility limit $\nu = 0.5$, where Eq. (B.9) predicts values 7% lower than Eq. (27).

In case of clamped ends, we can utilize the Saint Venant principle particularized for plates, since the horizontal and vertical flange of the T-beam can be modeled as thin plate strips. Since both horizontal and vertical flange of the T-beam have the same curvature, the influence of clamping is to provide an end moment and a self-equilibrated stress system that influences a length of the beam approximately $2e$ from the clamped end (Horgan and Knowles, 1983). The moment due to clamping will not change the picture of the above solution for the main part of the beam.

## Appendix C. Generalized derivative of the shear strain at the horizontal flanges of a T-beam

The generalized strain gradient of an antisymmetric field such as the shear strain at the horizontal flanges of a T-beam, with discontinuity at the origin, can be formulated by using the definition of the left Riemann–Liouville derivative of a function[4] $f(x)$,

$$ {}_xD_b^{\alpha} f(x) = (-1)^n \frac{\mathrm{d}^n}{\mathrm{d}x^n} {}_xI_b^{n-\alpha} f(x) \quad (n = \text{Integral part}(\alpha) + 1) \tag{C.1} $$

where the Riemann–Liouville fractional integral is defined as

$$ {}_aI_x^n f(x) = \frac{1}{(n-1)!} \int_a^x (x-u)^{n-1} f(u)\,\mathrm{d}u \tag{C.2} $$

As mentioned in the considered case the function at hand is discontinuous at the origin,

$$ \gamma_{xy} = \begin{cases} \gamma_R \\ \gamma_L \end{cases} = \frac{\tau_0}{G} \begin{cases} f_R = 1 + 2\psi & -1/2 \leqslant \psi < 0, \\ f_L = -1 + 2\psi & 0 < \psi \leqslant 1/2, \end{cases} \quad \psi = \frac{y}{b} \tag{C.3} $$

We define the generalized derivative of the above discontinuous shear strain distribution as the sum of 1st order the left Riemann–Liouville derivatives of both branches within the interval of interest,

$$ \bar{\kappa}_{xyy} = {}_yD_{-1/2}^{1} \gamma_R(y) + {}_yD_{1/2}^{1} \gamma_L(y) \tag{C.4} $$

with

$$ {}_yD_b^{\alpha} f(y) = \frac{1}{b} {}_{\psi}D_b^{\alpha} f(\psi) \tag{C.5} $$

It should be noted that the selection of the 1st order Riemann–Liouville derivative is due to the linearity of (C.3). Other functions may require different orders of the Riemann–Liouville derivative.

In the considered case we have

$$ {}_{\psi}D_{-1/2}^{1} f_R(\psi) = (-1)^2 \frac{\mathrm{d}^2}{\mathrm{d}x^2} {}_{\psi}I_{-1/2}^{2-1} f_R(\psi) = -\frac{\mathrm{d}^2}{\mathrm{d}x^2} {}_{-1/2}I_{\psi}^{1} f_R(\psi) \tag{C.6} $$

and

$$ {}_{\psi}D_{1/2}^{1} f_L(\psi) = (-1)^2 \frac{\mathrm{d}^2}{\mathrm{d}x^2} {}_{\psi}I_{1/2}^{2-1} f_L(\psi) = \frac{\mathrm{d}^2}{\mathrm{d}x^2} {}_{\psi}I_{1/2}^{1} f_R(\psi) \tag{C.7} $$

[4] Cf. Butzer and Westphal (2000).

Thus we get

$$
\begin{aligned}
{}_{-1/2}I^1_{\psi} f_R(\psi) &= \frac{1}{(1-1)!}\int_{-1/2}^{\psi}(\psi-u)^{1-1} f_R(u)\,\mathrm{d}u = \int_{-1/2}^{\psi}(1+2u)\,\mathrm{d}u = [u+u^2]^{\psi}_{-1/2} \\
&= \psi+\psi^2-\left(-\frac{1}{2}+\left(-\frac{1}{2}\right)^2\right) = \psi+\psi^2+\frac{1}{4}
\end{aligned}
\tag{C.8}
$$

and

$$
\begin{aligned}
{}_{\psi}I^1_{1/2} f_R(\psi) &= \frac{1}{(1-1)!}\int_{\psi}^{1/2}(\psi-u)^{1-1} f_L(u)\,\mathrm{d}u = \int_{\psi}^{1/2}(-1+2u)\,\mathrm{d}u = [-u+u^2]^{1/2}_{\psi} \\
&= \left(-\frac{1}{2}+\left(\frac{1}{2}\right)^2\right) - (-\psi+\psi^2) = -\frac{1}{4}+\psi-\psi^2
\end{aligned}
\tag{C.9}
$$

Thus

$$
{}_{\psi}D^1_{-1/2} f_R(\psi) = -\frac{\mathrm{d}^2}{\mathrm{d}x^2}\left(\frac{1}{4}+\psi+\psi^2\right) = -2 \tag{C.10}
$$

$$
{}_{\psi}D^1_{1/2} f_L(\psi) = \frac{\mathrm{d}^2}{\mathrm{d}x^2}\left(-\frac{1}{4}+\psi-\psi^2\right) = -2 \tag{C.11}
$$

and from Eqs. (C.4) and (C.5) we recover Eq. (27),

$$
\bar{\kappa}_{xyy} = \frac{\tau_0}{G}\frac{1}{b}(-4) \tag{C.12}
$$

In that sense $\bar{\kappa}_{xyy}$ is constant along the flanges of the T-beam. This result is also in accordance with Eq. (37).

## References


Bardet, J.-P., Vardoulakis, A., 2001. The asymmetry of stress in granular media. Int. J. Solids Struct. 38, 353–367.

Butzer, P.L., Westphal, U., 2000. An Introduction to Fractional Calculus. In: Hilfer, R. (Ed.), Applications of Fractional Calculus in Physics. World Scientific, Singapore.

Mindlin, R.D., 1964. Microstructure in linear elasticity. Arch. Rat. Mech. Anal. 10, 51–77.

Horgan, C.O., Knowles, J.K., 1983. Recent developments concerning Saint Venant's Principle. Adv. Appl. Mech. 23, 179–269.

Papargyri-Beskou, S., Tsepoura, K.G., Polyzos, D., Beskos, D.E., 2003. Bending and stability analysis of gradient elastic beams. Int. J. Solids Struct. 40, 385–400.

Timoshenko, S.P., 1921. On the correction for shear of the differential equation for transverse vibrations of prismatic beams. Philos. Mag. Sec. 6. 41, 744–746.

Timoshenko, S.P., Goodier, J.N., 1970. Theory of Elasticity, third ed. McGraw-Hill, New York.

Yeo, I.-S., Ho, P.S., Anderson, S.G.H., 1995. Characteristics of thermal stresses in Al (Cu) fine lines I. Unpassivated line structures. J. Appl. Phys. 78, 945–952.